Single-Crystal High-Frequency Electron Paramagnetic Resonance Investigation of a Tetranuclear Iron(III) Single-Molecule Magnet

August Bouwen,[†] Andrea Caneschi,[‡] Dante Gatteschi,*[,‡] Etienne Goovaerts,[†] Dirk Schoemaker,[†] Lorenzo Sorace,[‡] and Mariana Stefan[†,§]

Department of Physics, University of Antwerp (UIA), Universiteitsplein 1, 2610 Antwerp, Belgium, Department of Chemistry, University of Florence, Via Maragliano 77, 50144 Florence, Italy, and Institute of Atomic Physics (NIMP), POB MG-7 Magurele, 76900 Bucharest, Romania

Received: September 23, 2000; In Final Form: January 4, 2001

A high-frequency (95 GHz) electron paramagnetic resonance (EPR) study is reported on single crystals of the planar tetranuclear complex $Fe_4(OCH_3)_6(dpm)_6$ (where Hdpm = dipivaloylmethane), which has been previously shown to present typical single-molecule magnet behavior. The spectra, all originating from the $S = 5$ ground state, possess quasi-axial symmetry along the normal to the plane defined by the four Fe(III) ions. The measured spectra are shown to belong to three different structural variations of the compound, resulting from disorder in the ligands around two of the Fe(III) ions. Accurate values could be obtained for the second- and fourth-order crystal field parameters related to the parallel EPR spectra, while the other parameters could be determined only for the dominant species. The separation between individual lines is decreasing and vanishing with increasing temperature. This effect is attributed to the contribution of fast relaxing excited states, whose population is varying with temperature.

Introduction

Magnetic clusters of transition metal ions have been shown to exhibit so-called single-molecule magnet, SMM, behavior, in which magnetic bistability is observed at the level of a single molecule with very slow relaxation of the magnetization at very low temperatures.[1−13] The long relaxation time is determined by a high spin ground state and large Ising-type magnetic anisotropy, reflected in large and negative values of the axial zero-field splitting (zfs) parameter *D*. Several different systems are now known to exhibit SMM behavior. An appealing feature of these molecules is that they show quantum tunneling of the magnetization.[14−19] This is directly related to the splitting of the *S* multiplet, and therefore detailed knowledge of the energies of the M_s states is required for a deeper analysis of this phenomenon. Electron paramagnetic resonance (EPR) spectroscopy is the method of choice for the accurate determination of the magnetic properties of transition metal complexes. However, in the case of single-molecule magnets, with large zfs of the order of 1 cm^{-1}, it is necessary to apply high-frequency (high-field) EPR techniques at microwave frequencies of the order of 100 GHz or higher. In this way, detailed information has been gathered on the magnetic parameters and the relaxation dynamics of these systems.[20−25]

The relatively small cluster $Fe_4(OCH_3)_6(dpm)_6$ (where Hdpm = dipivaloylmethane)—Fe4 for simplicity—is characterized by an $S = 5$ ground state arising from antiferromagnetic interactions between central and peripheral iron spins and by an Ising-type magnetic anisotropy.[9] HF-EPR powder spectra indicated $D = -0.2$ cm^{-1} and $E < 0.02$ cm^{-1}. AC susceptibility measurements showed SMM behavior below 1 K, while Mössbauer spectra revealed slow relaxation of the magnetization below ca. 35 K.[26] Preliminary measurements have shown the typical stepped behavior of hysteresis loops due to resonant quantum tunneling, with the position of the steps in good agreement with the zfs value. Below 0.1 K the hysteresis loops became almost temperature-independent, suggesting that the relaxation occurred through a direct ground-state tunneling process between the $M_S = \pm 5$ states.[27]

The crystalline structure of the compound was determined to be monoclinic, with the space group *C*2/*c*. The individual molecules have 2-fold symmetry around the *b* axis, with the four Fe(III) ions lying in the same plane (Figure 1). The normal to the plane makes an angle of 2.1° with the *c* direction. As the intermolecular distances are larger than 9 Å, the intermolecular interactions are expected to be very weak, thus supporting the assumption that the magnetic behavior is deriving from the properties of the single molecule.

This simple structure is of particular interest from the perspective of reaching a detailed description of the magnetic parameters starting from the molecular structure and the single-ion properties. Even though the peculiar features of a SMM were well-established for Fe4, earlier powder HF-EPR spectra left us with large uncertainties about the actual value of the spin Hamiltonian parameters. To push further the characterization of the magnetic ground state, we decided to perform a single-crystal HF-EPR study on this system. The values of the zfs parameters determined from the HF-EPR powder spectra suggested the possibility of carrying on this investigation at W band (94 GHz), where all the features of the spectrum are shown. A well-defined advantage of W-band spectrometers is their sensitivity, which, due to the presence of a resonant cavity, is much higher than that currently available at higher frequencies. This allows the use of tiny single crystals, $0.4 \times 0.4 \times 0.4$ mm^3. The single-crystal analysis provided evidence for the principal directions of the zfs tensor and it confirmed the presence of three disordered sites in the unit cell. These had

[†] University of Antwerp.
[‡] University of Florence.
[§] Institute of Atomic Physics.

10.1021/jp003441d CCC: $20.00
Published on Web 03/14/2001

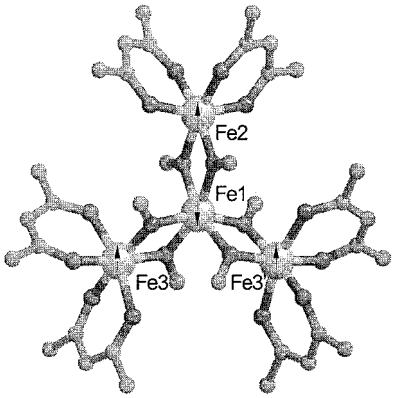

Figure 1. Structure of the Fe4 cluster. The arrows indicate the spin structure arising form the antiferromagnetic coupling of the central iron with the external ones.

been previously observed in the X-ray structure analysis,[9] but the EPR data provide direct access to the spin Hamiltonian parameters of the three disordered sites. These data can be important for the interpretation of the relaxation behavior of the magnetization of Fe4 at low temperatures.

Experimental Section

Prismatic single crystals of $Fe_4(OCH_3)_6(dpm)_6$ were prepared as described in ref 9, and any possible twinning was excluded after collection of low-θ frames with a Siemens-CCD diffractometer. The relative orientation of the crystallite facets was carefully determined after the collection of 25 reflections on a CAD4 Enraf Nonius four-circle diffractometer, equipped with graphite monochromated Mo Kα radiation.

The measurements were performed with a continuous-wave W-band EPR spectrometer (Bruker E600) with cylindrical cavity operating at 94 GHz, equipped with a split-coil superconducting magnet (Oxford) mounted on a rotating base. Both the sample holder and the magnet could be rotated around a vertical axis. The temperature variation was achieved with a continuous-flow cryostat (Oxford CF935 dynamic), operating from room temperature (RT) down to 4.2 K.

For W-band experiments, the oriented single crystals were mounted on silica-grade tubes with 0.9 mm outer diameter, embedded either in silicon grease or in glue, to have them well fixed and to protect them from the surrounding atmosphere. The crystals were either stuck onto the flat polished bottom of the tubes or on a flat polished side, along the vertical axis of the tube, to obtain the desired orientations (see Figure 2). Orientational errors of up to 5° can occur due to the visual procedure of alignment.

Single-crystal EPR studies were performed also at X-band (9.4 GHz), in a Bruker ESP 300E spectrometer equipped with a continuous-flow cryostat (Oxford ESR910) for temperature variations from RT down to 2.4 K. Eventually, several oriented crystals were mounted together on the sample holder in order to increase the signals. Correspondence of the resulting spectra with real single-crystal measurements was checked. The same precautions of protecting the crystals from deterioration by covering them with silicon grease were taken.

Polycrystalline powder EPR spectra were measured at X-band (9.23 GHz) with a Varian ESR9 spectrometer, equipped with a ^{4}He continuous-flow cryostat. To avoid preferential orientation, ground crystallites of Fe4 were embedded in wax.

The analysis of the spectra and the simulations were performed with a dedicated computer program.[28,29]

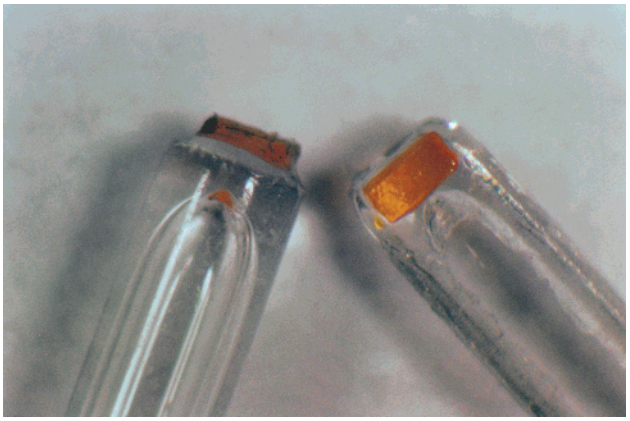

Figure 2. Fe4 single crystals mounted for W-band measurements in the *bc* plane (on the bottom of the tube) and *a***c* plane (on the side), respectively. The tube outer diameter is 0.9 mm.

Results and Discussion

As a consequence of the molecular structure, *b* is necessarily one of the magnetic axes, and the analysis of the spectra recorded in the *a***c* plane directly leads to the identification of the two remaining magnetic axes. The maximum width of the W-band EPR spectrum in this plane (see Figure 3a) has been clearly observed close to the *c* direction, while it is minimal along *a**. Due to the experimental errors it was not possible to distinguish the crystallographic *c* axis from the normal to the plane defined by the four iron(III) ions. We may conclude that, within the experimental errors, the crystallographic *c* axis is the easy axis of the magnetization, while *a** is the third magnetic axis. It should be noticed that these results are essentially in agreement with the predictions obtained through an angular overlap approach in ref 9.

The angular variation of the spectra measured at $T = 25$ K in the *a***c* and *bc* planes (see Figure 3) clearly shows the characteristic features of a quasi-axial $S = 5$ center: 10 approximately equidistant transitions along the *c* direction ($\theta = 0°$) are nearly collapsing to one line upon rotation to the magic angle (54.74°) and yield a pattern of near-equidistant lines with half the splitting in the *a** and *b* directions ($\theta = 90°$). The negative sign of *D* obtained from the powder HF-EPR study[9] is confirmed by the observation of the effects due to population distribution, with higher intensities for the low-field lines in the parallel spectra relative to the high-field ones and the opposite effect in the perpendicular spectrum. This becomes even more obvious in the $T = 5$ K spectra (see Figure 4), in which the high-field lines are vanishing for the parallel direction, as well as the low-field lines in the perpendicular orientation. The observed line−line separations are consistent with the already reported value of $D = -0.2$ cm^{-1}. Another feature is most clearly observed in the low-temperature spectrum with the field parallel to *c* (Figure 4) but also at higher temperatures: each of the EPR lines is composite and consists of three transitions—two of nearly equal intensity and a weaker one—which we attribute to three different paramagnetic centers with similar properties but slightly different *D* values. The observation of three centers can be directly related to the three isomers known to occur for the studied compound. Indeed, a random disorder was found in the coordination environment of Fe3, consisting of a 0.30 occupancy of the dpm ligands in a different spatial arrangement with respect to the dominant one. To illustrate this, we refer to the overall structure of the Fe/O core, which comprises two parallel layers of c.p. oxygen atoms (maximum deviation 0.26 Å), one on each side of the Fe4

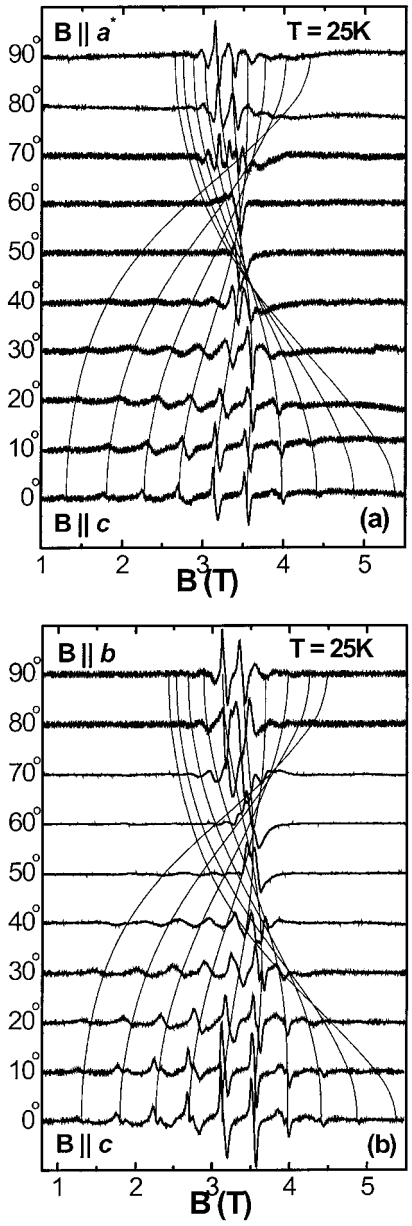

Figure 3. Angular variation of the Fe4 W-band EPR single-crystal spectra at 25 K in the *a***c* plane (a) and the *bc* plane (b). The solid lines are the calculated angular dependence with the parameters for center AA from Table 1.

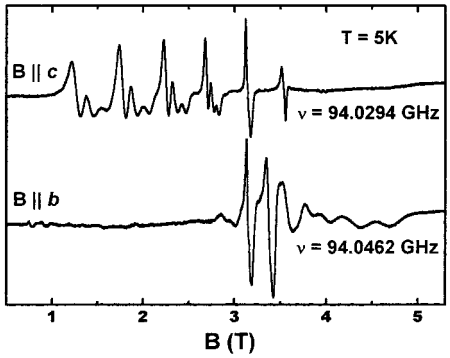

Figure 4. W-band EPR single-crystal spectra at 5 K along the parallel (∼*c* axis) and perpendicular directions (*b* axis), respectively.

moiety. Each of the two dpm anions can provide two oxygen donors either on different (mode A) or on the same oxygen layers (mode B). Since the coordination sphere of Fe2 is not

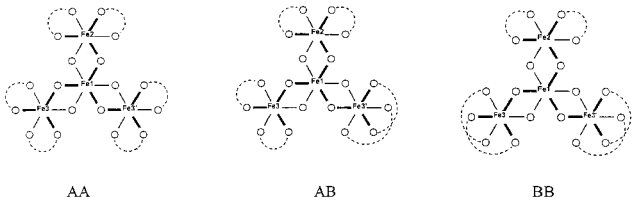

Figure 5. Scheme of the three isomers AA, AB, and BB, showing the different binding modes of the dpm anions on Fe3 and Fe3′.

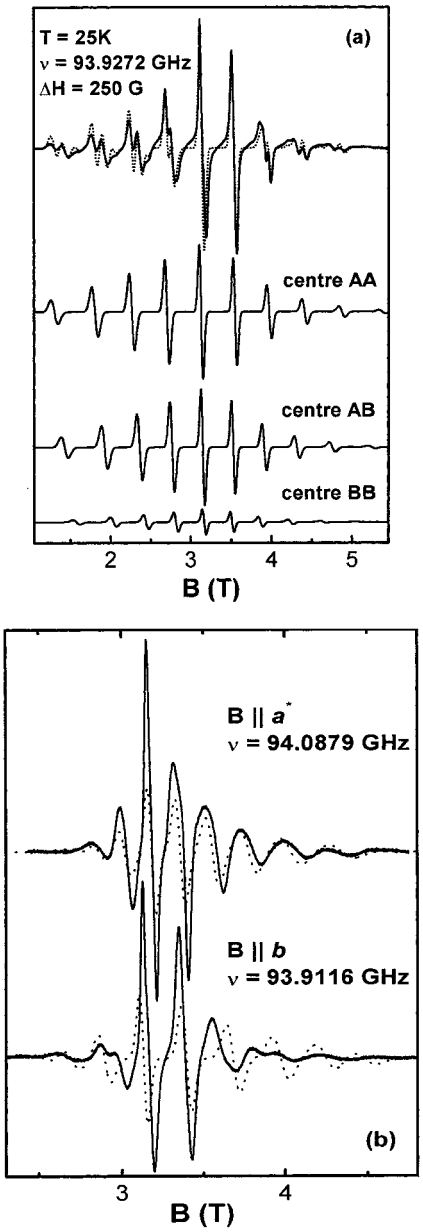

Figure 6. (a) W-band EPR spectrum along the *c* axis at 25 K; simulated spectra for the three isomers using the parameters from Table 1 and the intensity ratios 0.49:0.42:0.09. The dotted line is the sum of the three calculated spectra. (b) W-band EPR spectra along the *a** and *b* axes, respectively, at 25 K, together with the simulated spectra for center AA (dotted lines) with the parameters from Table 1.

disordered, we can conclude that the crystal is essentially a mixture of three isomers corresponding to AA, AB, and BB combinations on the Fe3 and Fe3′ sites (see Figure 5), with expected occupancies 0.49, 0.42, and 0.09, respectively. In Figure 6a, it is shown that the spectrum recorded at 25 K with the magnetic field parallel to *c* is quite well simulated with these

TABLE 1: Spin-Hamiltonian Parameters for the Three Different Isomers Occurring in the *Fe4* Crystals

parameter	center AA	center AB	center BB
g_x	1.995 ± 0.005		
g_y	1.997 ± 0.005		
g_z	2.009 ± 0.005	2.009 ± 0.005	2.009 ± 0.005
D (cm^{-1})	-0.206 ± 0.001	-0.190 ± 0.002	-0.175 ± 0.002
E (cm^{-1})	0.010 ± 0.003		
B_4^0 (cm^{-1})	$-(1.1 \pm 0.2) \times 10^5$	$-(1.6 \pm 0.2) \times 10^5$	$-(1.6 \pm 0.2) \times 10^5$
B_4^2 (cm^{-1})	$-(0.8 \pm 0.3) \times 10^4$		
B_4^4 (cm^{-1})	$-(0.4 \pm 0.3) \times 10^4$		

ratios for the intensities of the three spectra. By passing from the AA to the AB center contribution, a reduction (nearly 8%) in D is observed (see Table 1). This is about doubled (to 15%) when both sites are in the B-mode.

A clear identification of the transition fields belonging to different centers was possible only along the parallel direction (Figures 4 and 6a). The distances between neighboring lines are not equal to each other, increasing from the center of the spectrum to the extremes. This suggests that contributions from higher order terms in the crystal field interactions are of nonnegligible importance. We then employed for simulations a complete fourth-order Hamiltonian:

$$H = \beta SgB + DS_z^2 + E(S_x^2 - S_y^2) + B_4^0 O_4^0 + B_4^2 O_4^2 + B_4^4 O_4^4 \quad (1)$$

where[30]

$$O_4^0 = 35S_z^4 - 30S(S+1)S_z^2 + 25S_z^2$$

$$O_4^2 = \{[7S_z^2 + S(S+1) - 5](S_+^2 + S_-^2) + (S_+^2 + S_-^2)[7S_z^2 + S(S+1) - 5]\}/4$$

$$O_4^4 = (S_+^4 + S_-^4)/2$$

The parameters g_z, D, and B_4^0, which essentially determine the line positions in the parallel spectrum, could be accurately determined for all three centers (see Table 1). The lines are quite broad and the line widths (peak-to-peak of the derivative) increase from the center toward the outermost peaks of the spectra from about 50 to 120 mT from the central to the extreme lines, i.e., from small to large $|M_S|$ values of the $S = 5$ states involved (Figures 4 and 6). This suggests a distribution in the D values resulting from a local strain-induced effect. A similar M_S dependence of the line width was previously observed in the single-crystal HF-EPR spectra of another SMM, namely, Fe8.[25] The line width broadening could be reasonably well simulated by considering a distribution in the values of the zero-field splitting parameters D and E around their average value, while the intensity ratio in the spectrum could be well reproduced by considering a Boltzmann factor with $T = 25$ K (see Figure 6a). The line broadening was simulated by consideration of broadening factors $f_1 = f_2 = 1.1 \times 10^{-5}$ cm^{-1}/T:

$$\Gamma = \Gamma_0(1 + f_1|dB_i/dD| + f_2|dB_i/dE|) \quad (2)$$

where Γ_0 is the line width in the absence of the broadening effect, Γ is the broadened line width, and B_i is the resonance magnetic field for a specific resonance.[28,29,31]

Within experimental accuracy, the maximum extent for all three spectra appeared along the same direction (the c direction). The calculated angular variation in Figure 3 is obtained from the refined spin-Hamiltonian parameters of the dominant center

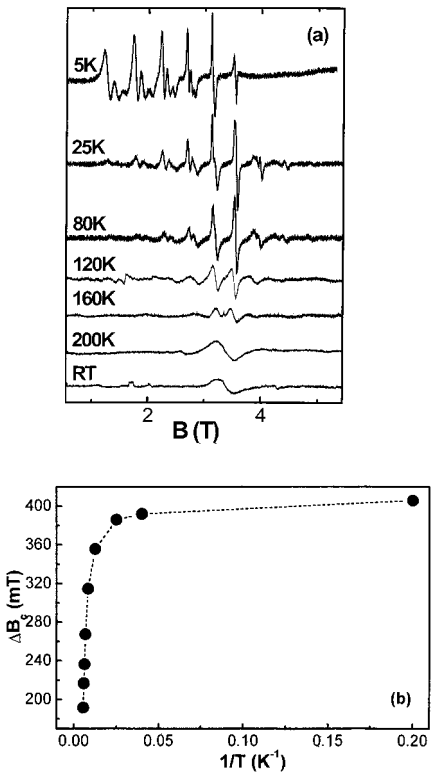

Figure 7. (a) Variation of the single-crystal spectrum along the c axis with temperature. (b) Variation of the separation between the central transitions ΔB_c with temperature. The dotted line is a guide for the eye.

AA. However, an angular variation in the perpendicular plane (a^*b) reveals a slight in-plane anisotropy (Figure 6b). Because of the overlap between lines and the large line widths, the transitions could not be univocally assigned to the three different centers. Approximate values could be determined for the orthorhombic parameters of the dominant isomer (see Table 1), assuming the three centers to be coaxial. This assumption cannot be expected to be entirely correct, as the only local symmetry element for the clusters is the b-axis. In fact, only the centers characterized by AA and BB combinations hold this symmetry axis, while for the AB-type centers even this symmetry is not valid anymore. Consequently, the different isomers, and in particular the AB-type centers, would have different principal axes of the interaction tensors, which would certainly add to the difficulty of the spin-Hamiltonian analysis.

Attempts were made also to record the X-band spectra of single crystals. In fact, the spectra and their angular variation could be measured and were visible up to 90 K, above which they became too broad and disappeared. Even at low temperature the lines are quite broad, from 185 G along the c direction up to 500 G along the b axis. Moreover, three overlapping spectra from the three isomers are expected. Probably for these reasons, the analysis was not feasible, even upon starting from the parameters derived from the W-band spectra, and no valuable information about the spin-Hamiltonian parameters could be extracted. This is again a confirmation of the important role of high-frequency EPR in the characterization of SMM.

With increasing temperature excited multiplets begin to be populated, since two $S = 4$ states and three $S = 3$ states are lying at only 37.1 and 76.1 cm^{-1} above the ground $S = 5$ states, respectively. In principle, additional spectra corresponding to these states might be observed. However, this is not the case in the single-crystal W-band spectra shown in Figure 7a.

In fact, with increasing temperature the lines become broader and the separation between the transition fields decreases, until above 200 K only a single broad line is observed at $g \approx 2$ (see Figure 7a). Figure 7b displays the temperature dependence of the distance between the two central lines, which result from the superposition of the lines belonging to the three centers. A similar temperature dependence of the resonance field positions has been reported for a family of Cu(II) trimers.[32] This behavior was attributed to the presence in the observed signal of contributions from different states. In this framework the decreasing of the line−line separation with increasing temperature for Fe4 could be attributed to the increasing contribution of higher spin states whose fast relaxation times, due to the large number of multiplets arising from the coupling of the four iron(III) ions, do not permit the observation of a spectrum. In agreement with the fast relaxation time of the excited multiplets no signal was found in the single-crystal spectra, at either W- or X-band, which could originate from a thermally populated excited spin manifold, despite careful temperature-dependent measurements. In a previous powder investigation,[9] an excited $S = 4$ state with much lower D value was invoked to explain both a central feature in the high-frequency spectra and a specific X-band spectrum. However, the new powder X-band spectra, whose features are in agreement with what was expected from the determined spin-Hamiltonian parameters, could not reproduce the earlier result. The latter seems to have originated from the presence of impurities such as the dimer $Fe_2(OMe)_2(dpm)_2$, a secondary product of the synthesis.

We were able to essentially reproduce the central features in the high-frequency (190 and 245 GHz) powder spectra first attributed to an excited state, using our refined spin-Hamiltonian parameters and taking into account the line width variations and the thermal population of the M_S states. This central feature is outstanding in the powder spectra at higher temperatures because of different reasons: the narrower width of the central transitions, the increasing population of the low $|M_S|$ states, and the extremes in the angular variation occurring in this region close to the magic angle (see Figure 3). Even in the single-crystal W-band spectra (Figure 3), the central lines have an unexpectedly high amplitude due to the first two of these effects.

Conclusions

The single-crystal W-band EPR spectra of Fe4 showed that the zfs of the ground $S = 5$ state is quasi-axial, the unique axis being approximately perpendicular to the plane of the four iron(III) ions. While the qualitative analysis of the spectra has been essentially confirmed by the simulations, these showed unequivocally that the assumption of a line broadening process, probably due to a D strain, is absolutely necessary to quantitatively reproduce the line width of the spectrum along the easy direction. This is then an additional parameter to be considered when interpreting HF-EPR spectra of SMM.

The presence of three structural variations previously observed in an X-ray analysis was also confirmed, and different values for the spin-Hamiltonian parameters of the three isomers could be determined. This may explain why simple calculations performed on an averaged structure allowed reconstruction of only about 30% of the experimental D value.[9] Presumably the differences in the zfs parameters may give rise to different blocking temperatures, as evidenced by the presence of different maxima in the χ' vs T plots.

The presence of minority species is now seen to be rather common in molecular clusters. In fact, by increasing the complexity of the molecular species it is increasingly possible to accommodate slightly different variants in the same lattice. Similar effects were previously observed by EPR in the case of isolated dimers[33] and now have been observed in the lattice of the archetypal SMM, Mn12Ac.[34] EPR, being a technique based on local probing, is extremely useful for monitoring the different structures.

Acknowledgment. We acknowledge A. Cornia for useful suggestions about the X-ray structure and R. Sessoli for stimulating discussions. Financial support from the Belgian National Fund for Scientific Research (FWO-Flanders) is gratefully acknowledged. E.G. is a Research Director of FWO. M.S. is grateful to European Science Foundation (ESF) for the grant accorded in the frame of the "Molecular Magnets" Scientific Program in order to perform part of these studies. Finally, the financial support of EC (Contract HPRN-CT-1999-00012), MURST, and Italian CNR are acknowledged.

References and Notes

(1) Sessoli, R.; Gatteschi, D.; Caneschi, A.; Novak, M. A. *Nature* (*London*) **1993**, *365*, 141−143.

(2) Taft, K. L.; Papafthymiou, G. C.; Lippard, S. J. *Science* **1993**, *259*, 1302.

(3) Eppley, H. J.; Tsai, H.-L.; de Vries, N.; Folting, K.; Christou, G.; Hendrickson, D. N. *J. Am. Chem. Soc.* **1995**, *117*, 301−317.

(4) Barra, A. L.; Debrunner, P.; Gatteschi, D.; Schulz, Ch. E.; Sessoli, R. *Europhys. Lett.* **1996**, *35*, 133−138.

(5) Aubin, S. M. J.; Wemple, M. W.; Adams, D. M.; Tsai, H.-L.; Christou, G.; Hendrickson, D. N. *J. Am. Chem. Soc.* **1996**, *118*, 7746.

(6) Castro, S. L.; Sun, Z. M.; Grant, C. M.; Bollinger, J. C.; Hendrickson, D. N.; Christou, G. *J. Am. Chem. Soc.* **1998**, *120*, 2365−2375.

(7) Pilawa, B.; Kelemen, M. T.; Wanka, S.; Geisselmann, A.; Barra, A. L. *Europhys. Lett.* **1998**, *43*, 7−12.

(8) Brechin, E. K.; Yoo, J.; Nakano, M.; Huffman, J. C.; Hendrickson, D. N.; Christou, G. *J. Chem. Soc., Chem. Commun.* **1999**, 783−784.

(9) Barra, A. L.; Caneschi, A.; Cornia, A.; De Biani, F. F.; Gatteschi, D.; Sangregorio, C.; Sessoli, R.; Sorace, L. *J. Am. Chem. Soc.* **1999**, *121*, 5302−5310.

(10) Barra, A. L.; Caneschi, A.; Gatteschi, D.; Goldberg, D. P.; Sessoli, R. *J. Solid State Chem.* **1999**, *145*, 484−487.

(11) Oshio, H.; Hoshino, N.; Ito, T. *J. Am. Chem. Soc.* **2000**, *122*, 12602.

(12) Gatteschi, D.; Sessoli, R.; Cornia, A. *J. Chem. Soc., Chem. Commun.* **2000**, 725−732.

(13) Christou, G.; Gatteschi, D.; Hendrickson, D. N.; Sessoli, R. *MRS Bull.* **2000**, *25*, 66.

(14) Thomas, L.; Lionti, F.; Ballou, R.; Gatteschi, D.; Sessoli, R.; Barbara, B. *Nature* (*London*) **1996**, *383*, 145−147.

(15) Friedman, J. R.; Sarachik, M. P.; Tejada, J.; Ziolo, R. *Phys. Rev. Lett.* **1996**, *76*, 3830.

(16) Friedman, J. R.; Sarachik, M. P.; Tejada, J.; Maciejewski, J.; Ziolo, R. *J. Appl. Phys.* **1996**, *79*, 6031.

(17) Sangregorio, C.; Ohm, T.; Paulsen, C.; Sessoli, R.; Gatteschi, D. *Phys. Rev. Lett.* **1997**, *78*, 4645−4648.

(18) Caneschi, A.; Gatteschi, D.; Sangregorio, C.; Sessoli, R.; Sorace, L.; Cornia, A.; Novak, M. A.; Paulsen, C.; Wernsdorfer, W. *J. Magn. Magn. Mater.* **1999**, *200*, 182−201.

(19) Chudnovsky, E. M.; Tejada, J. *Macroscopic Quantum Tunneling of the Magnetic Moments;* Cambridge University Press: Cambridge, U.K., 1998.

(20) Barra, A. L.; Caneschi, A.; Gatteschi, D.; Sessoli, R. *J. Am. Chem. Soc.* **1995**, *117*, 8855−8856.

(21) Barra, A. L.; Gatteschi, D.; Sessoli, R. *Phys. Rev. B*: *Condens. Matter* **1997**, *56*, 8192−8198.

(22) Barra, A. L.; Brunel, L. C.; Gatteschi, D.; Pardi, L.; Sessoli, R. *Acc. Chem. Res.* **1998**, *31*, 460−466.

(23) Aubin, S. M. J.; Dilley, N. R.; Pardi, L.; Krzystek, J.; Wemple, M. W.; Brunel, L. C.; Maple, M. B.; Christou, G.; Hendrickson, D. N. *J. Am. Chem. Soc.* **1998**, *120*, 4991−5004.

(24) Aubin, S. M. J.; Sun, Z. M.; Pardi, L.; Krzystek, J.; Folting, K.; Brunel, L.-C.; Rheingold, A. L.; Christou, G.; Hendrickson, D. N. *Inorg. Chem.* **1999**, *38*, 5329.

(25) Barra, A. L.; Gatteschi, D.; Sessoli, R. *Chem.—Eur. J.* **2000**, *6*, 1608−1614.

(26) Caneschi, A.; Cianchi, L.; Del Giallo, F.; Gatteschi, D.; Moretti, P.; Pieralli, F.; Spina, G. *J. Phys.*: *Condens. Matter* **1999**, *11*, 3395−3403.

(27) Sessoli, R.; Caneschi, A.; Sorace, L.; Cornia, A.; Wernsdorfer, W. *J. Magn. Magn. Mater.* **2001** (in press).
(28) Glerup, J.; Weihe, H. *Acta Chem. Scand.* **1991**, 444.
(29) Jacobsen, C. J. H.; Pedersen, E.; Villadsen, J.; Weihe, H. *Inorg. Chem.* **1993**, *32*, 1216.
(30) Abragam, A.; Bleaney, B. *Electron Paramagnetic Resonance of Transition Ions;* Dover Publications: New York, 1986.
(31) Pilbrow, J. R. *Transition Ion Electron Paramagnetic Resonance*; Oxford University Press: Oxford, U.K., 1990.
(32) Fleischhauer, P.; Gehring, S.; Saal, C.; Haase, W.; Tomkowicz, Z.; Zanchini, C.; Gatteschi, D.; Davidov, D.; Barra, A. L. *J. Magn. Magn. Mater.* **1996**, *159*, 166−174.
(33) Bencini, A.; Gatteschi, D.; Zanchini, C.; Kahn, O.; Verdaguer, M.; Julve, M. *Inorg. Chem.* **1986**, *25*, 3181.
(34) Wernsdorfer, W.; Sessoli, R.; Gatteschi, D. *Europhys. Lett.* **1999**, *47*, 254−259.